Visible-Light Initiated Dispersion Photopolymerization of Styrene

Rémi Canterel, Jacques Lalevée, Elodie Bourgeat-Lami, Emmanuel Lacôte, Muriel Lansalot

RESEARCH ARTICLE

Visible-Light Initiated Dispersion Photopolymerization of Styrene

Rémi Canterel,[a,b] Jacques Lalevée,[c,d] Elodie Bourgeat-Lami,*[a] Emmanuel Lacôte,*[b] Muriel Lansalot*[a]

Dedicated to our colleague and friend Prof. Shigeru Yamago on the occasion of his 60th birthday.

[a] Dr. R. Canterel, Dr. E. Bourgeat-Lami, Dr. M. Lansalot,
Univ Lyon, Université Claude Bernard Lyon 1, CPE Lyon, CNRS, UMR 5128, Catalysis, Polymerization, Processes and Materials (CP2M), 43 Bd du 11 novembre 1918, F-69616 Villeurbanne, France
E-mail: elodie.bourgeat-lami@univ-lyon1.fr ; muriel.lansalot@univ-lyon1.fr
[b] Dr. R. Canterel, Dr. E. Lacôte
Univ Lyon, Université Claude Bernard Lyon 1, CNRS, CNES, ArianeGroup, LHCEP, Bât. Raulin, 2 rue Victor Grignard, F-69622 Villeurbanne, France
E-mail: emmanuel.lacote@univ-lyon1.fr
[c] Prof. J. Lalevée
Université de Haute-Alsace, CNRS, IS2M UMR 7361, F-68100 Mulhouse, France
[d] Université de Strasbourg, France

Supporting information for this article is given via a link at the end of the document.

Abstract: Polystyrene (PS) particles were synthesized in ethanol/water mixture by dispersion polymerization using visible light irradiation, with either a *N*-heterocyclic carbene borane-based photoinitiating system (PIS) or a disulfide. With the full PIS and poly(ethylene glycol) methyl ether methacrylate (PEGMA) as stabilizer, the size distributions were broad and the amount of PEGMA had a strong impact on the experiment reproducibility. The addition of a base solved the problem, leading to faster polymerizations, narrower size distributions and larger particles. With the disulfide as sole PIS, bigger and narrowly distributed PS particles were again formed. Quantitative conversion was achieved in each system, with particle size ranging between 100 and 350 nm. The use of poly(*N*-vinylpyrrolidone) as stabilizer led to significantly larger particles, up to 1.2 µm, with narrow size distributions. The production of such large latex particles by photoinitiated polymerizations is unprecedented.

Introduction

The use of light to generate polymer particles has been the focus of recent intense efforts, both in step-growth[1-3] and radical polymerizations.[4] For the latter, combining the strengths of photopolymerization (temporal and spatial control) with those of radical polymerization in dispersed (mostly aqueous) media – first and foremost the formation of low viscosity products even at high polymer contents – has been a goal for the past 45 years. The use of light to initiate polymerizations in dispersed media was examined first for emulsion polymerization.[5-7] Most studies initially relied on UV light, which however does not penetrate well in the turbid reaction media associated with such processes. Micro- and miniemulsion systems have been implemented to overcome this limitation.[4] These processes feature smaller-sized monomer droplets and final particles, which limits the scattering and the absorption of the UV photons and enhanced light penetration.

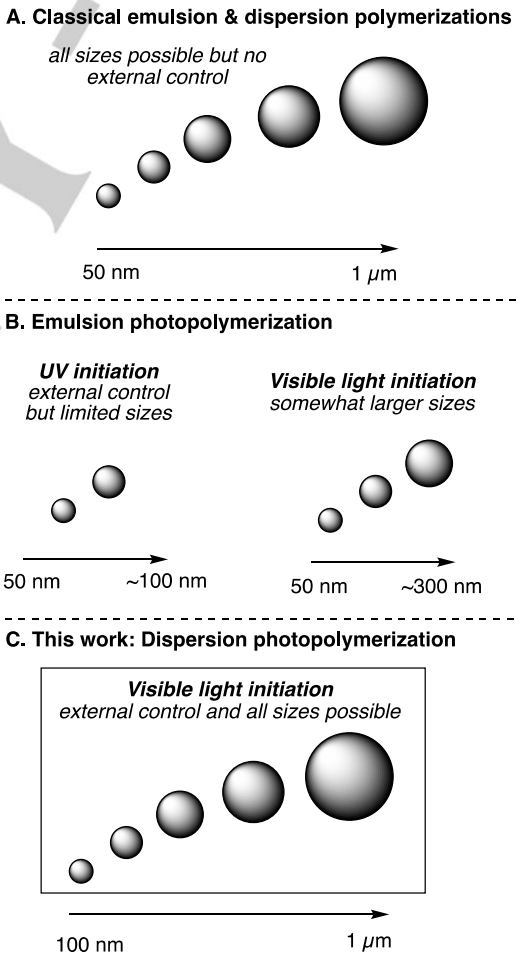

Figure 1. Particle-size ranges accessible in dispersed media using classical redox or thermal conditions (A), UV (B, left), visible-light (B, right) initiation in emulsion, and visible-light dispersion photopolymerizations (this work, C).

However, this limits the methods to the formation of smaller particles (~100 nm), where classical dispersed media processes can deliver particles up to the micrometer scale (Figure 1A and 1B, left). Besides, UV light is highly energetic, hazardous and requires specific equipment and glassware.

This spurred the development of visible light photoinitiating systems (PISs) that can have the advantage of improved light penetration.[8-16] We showed that a *N*-heterocyclic carbene (NHC) borane-based PIS led to very stable latexes of polystyrene (PS) or poly(meth)acrylates by aqueous emulsion polymerization with solids contents up to 30%.[17-18] The key step is the formation of an initiating boryl radical via hydrogen atom abstraction from a NHC-borane co-initiator by a photogenerated thiyl radical. The diameter of the particles obtained ranged from 50 to 300 nm (Figure 1B, right). However, the different components of the PIS and intermediates partitioned between the different phases of the system (water, monomer droplets and particles) resulting in some cases in broad particle size distributions. Also, due to the presence of the monomer droplets and/or micelles at the beginning of the reaction, then of the growing particles, the photons might still be subject to scattering effects – especially by larger-sized particles, thus limiting the penetration of light in the depth of the reactor and therefore the availability of initiating radicals.

In the present work, we report the transposition of our photoinitiating system to dispersion photopolymerizations (Figure 1C). In dispersion polymerizations all the components (monomer, initiator, and macromolecular stabilizer) are initially soluble in the solvent system. This homogeneous phase enables unfettered light penetration in the early stages of the reaction. The polymer produced is however insoluble and precipitates into particles stabilized by the steric/macromolecular stabilizer, which prevents their aggregation. Depending on the initial conditions, the particles can cover a broad range of sizes, typically between 100 nm and the micrometer scale.[19]

When the first polymer particles are formed however, the polymerization can take place in both the continuous phase and the particles. The competition between these two polymerization loci depends on the solvency of the reagents and intermediates in the continuous phase – which varies throughout the polymerization, the partitioning of these species, or the particle size. The reaction rate thus results from a combination of polymerization in the continuous phase and polymerization inside the swollen polymer particles. From the photopolymerization standpoint, light penetration – and therefore rates – will be further affected by the formation of polymer particles.

Photoinitiation under conventional dispersion conditions remains quite scarce in the literature, and UV photons are generally used.[20-22] Most recent efforts have focused on polymerization-induced self-assembly (PISA).[15, 23-25] In these systems, which often use visible light sources, a living solvophilic macromolecule is used to polymerize a solvophilic monomer to form diblock copolymers that self-assemble *in situ* to generate a diverse set of nano-objects. The mechanism of particle formation is therefore different from that of a conventional dispersion polymerization.

Our aims in this study were i) to move regular dispersion photopolymerization toward using safer and greener LED light sources, as we did for emulsion; ii) to determine whether the initial transparency of the reaction medium could be beneficial to radical production – and conversely whether this is the limiting factor we observed in emulsion photopolymerizations; iii) by changing the mechanism of polymer formation, to break the ~300 nm diameter ceiling observed for the particles produced via photo-emulsion.

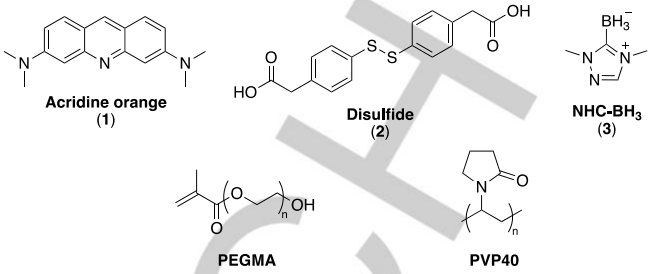

Figure 2. Chemical structure of the PIS and the two steric stabilizers, PEGMA and PVP40, used for the dispersion photopolymerization of styrene under visible light irradiation.

Results and Discussion

Our PIS is composed of acridine orange (**1**), an ω–ω′ dicarboxylic acid aryl disulfide (**2**) and 2,4-dimethyl-1,2,4-triazol-3-ylidene borane (NHC-BH_3, **3**, Figure 2).[17-18] All styrene polymerizations were performed in a ethanol/water mixture (70/30 wt/wt). We selected the poly(ethylene glycol) methyl ether methacrylate macromonomer PEGMA (ca. 2 000 g mol^{-1}) and the poly(*N*-vinylpyrrolidone) polymer (PVP40, ca. 40 000 g mol^{-1}) as stabilizers. The experiments were carried out in a double-wall glass reactor equipped with a LED ribbon coiled around the external glass walls (see the Supporting Information for details).

Preliminary experiments. In a first experiment, styrene was mixed in a polymerization reactor with the ethanol/water mixture (10 wt.% with respect to the solvents) in the presence of PEGMA (18 wt.% based on monomer), NHC-borane **3** (1.3 10^{-3} mol L^{-1}, based on solvent), disulfide **2** (50 mol% with respect to **3**) and **1** (1 mol% with respect to **3**). The resulting solution was de-aerated by bubbling nitrogen, then irradiated using a white LED garland[18] strapped on the exterior wall of the reactor (temperature controlled at 40 °C) and the reaction was followed by gravimetric analysis (Table 1, Run 1). PEGMA is a macromonomer commonly used in traditional styrene dispersion polymerization. It forms *in situ* graft copolymers, which strongly adsorb onto the particle surface.[26-31] The conversion reached approximately 90% after 24 h irradiation and the latexes obtained were stable without any coagulum. The reaction was repeated twice (runs 2-3) and the results and kinetic profiles of the polymerizations were similar (Figure 3a).

The average hydrodynamic particle diameters (D_h) of the final latexes measured by DLS were similar (180 nm) and reasonably low polydispersity indexes (PdI ≤ 0.07) were obtained. However, the number-average particle diameters determined from TEM analyses (D_n) were lower, and the corresponding size histograms show broader particle size distributions (Figures 3b and S2). That is due to the fact that DLS tends to overestimate the presence of larger objects. The molar masses obtained at the end of the polymerizations were again similar, confirming the reproducibility of these experiments (Table 1).

The time-conversion curves exhibit a profile characteristic of an auto-acceleration phase (around 15% conversion), followed by a deceleration of the polymerizations after 60% conversion. The

former could be the result of both a higher radical capture and a relatively low monomer concentration in the particles resulting in a high internal viscosity, and hence a lower probability of radical termination.[26, 31-34] In addition, the three-component PIS may partition between the continuous phase and the monomer-swollen particles, and therefore, it is also possible that the generation of radicals can occur in the polymer particles, which may accelerate the polymerization. The slowing down of the polymerization after 60 % conversion is likely a consequence of the reduced styrene concentration in the polymer particles as well as in the continuous phase. Moreover, the turbidity increased with the conversion, gradually limiting the light penetration inside the vessel. This could reduce the efficiency of our PIS.

As reported in the literature,[29-30, 35-36] the use of a macromonomer should enhance the stabilization of the particles and rapidly fix the number of particles, thus leading to narrow particle size distributions (PSDs). However, we observed relatively broad PSDs (D_w/D_n = 1.1). In our system the reaction starts from a homogeneous solution containing the full PIS, styrene, and PEGMA. The radicals generated from the PIS add to styrene units and form oligomers that precipitate when they reach a critical chain length. Enough graft copolymer chains of P(styrene-*g*-PEGMA) are likely formed at the same time to stabilize the primary particles, but we believe that the photoinduced initiation step produces radicals rather slowly and continuously, leading to a slow and continuous nucleation (as already observed in emulsion polymerization,[17] Figure S3), which would broaden the size distribution. The slower consumption of PEGMA with respect to styrene[26, 31, 37] and its relatively high concentration (18 wt.% versus < 2 wt.% for instance in ref [30-31]) could also contribute to the broad PSD because the probability for a new radical to generate a new particle relative to entering an already existing one is higher at higher stabilizer concentration.

Table 1. Visible-Light Dispersion Photopolymerizations of Styrene with the NHC-Borane-Based PIS.

Run [a]	PEGMA (wt.%)	Time (h)	Conv. (%)	D_h (nm)[b]	PdI[b]	N_p (10^{13} cm^{-3}) [c]	D_n (nm) [d]	D_w/D_n [d]	N_p (10^{13} cm^{-3}) [e]	M_n (kg mol^{-1}) [f]	$Đ$ [f]
1	18	23.7	92	182	0.02	2.5	152	1.09	4.3	91	5.1
2	18	24.6	90	184	0.07	2.2	143	1.10	4.6	87	4.9
3	18	22.3	82	150	0.02	3.6	118	1.10	7.4	78	6.2
4	25	22.3	97	131	0.05	6.6	97	1.12	16.3	104	3.8
5	10	21.8	88	204	0.06	1.6	207	1.19	1.5	58	5.9
6	5	23.7	98	470	0.17	0.2	345	1.25	0.4	40	9.3
7	2.5	23.5	100	577	0.05	0.4	340	1.15	0.4	32	7.7
8[g]	18	8.1	82	349	0.09	0.3	337	1.02	0.3	200	4.1
9	10	22.7	56	189	0.08	1.3	n. d.	n. d.	n. d.	52	7.0
10	10	28	88	192	0.03	2.0	202	1.06	1.7	60	5.4
11 [h]	10	6	96	245	0.07	1.0	246	1.02	0.4	116	4.7

[a] Conditions: the continuous phase was prepared by adding styrene (10 wt.% with respect to water and ethanol), the stabilizer (PEGMA), NHC-borane (1.3 10^{-3} mol L^{-1}), AO (1.3 10^{-5} mol L^{-1}, 1 mol%/NHC-BH_3), disulfide (6.3 10^{-4} mol L^{-1}, 50 mol%/NHC-BH_3) in ethanol/water (70/30 wt/wt). All concentrations are expressed per liter of solvents. [b] Hydrodynamic diameter and polydispersity index determined by DLS. [c] Number of particles calculated from D_h. [d] Number-average diameter and size dispersity determined by TEM. [e] Number of particles calculated from D_n (see SI for details). [f] Number-average molar mass and dispersity determined by SEC-THF. [g] Same conditions as run 1 except without NHC-borane and without AO. [h] Thermal initiation with AIBN, 1 wt.%/styrene at 70 °C.

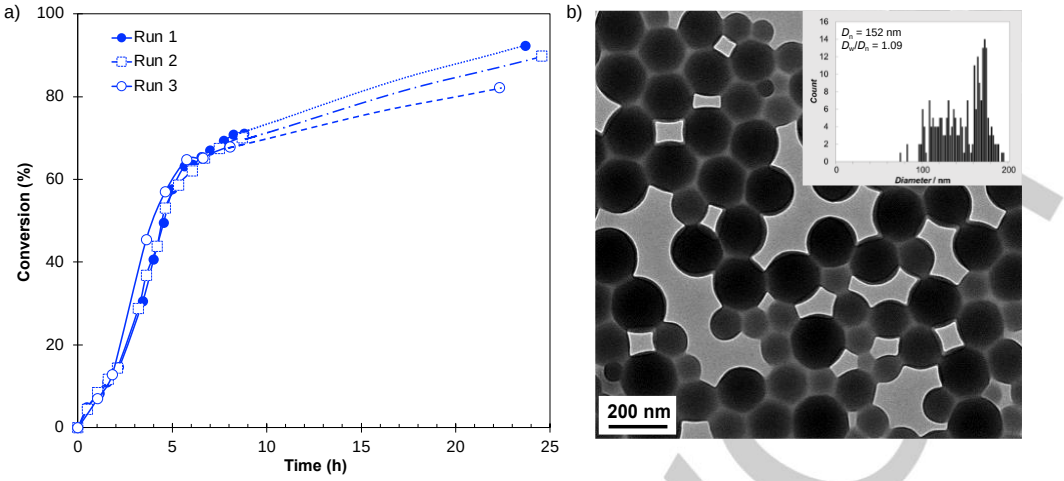

Figure 3. Reproducibility – a) Evolution of conversion with time for dispersion photopolymerization of styrene with the stabilizer PEGMA, 18 wt.% based on styrene. b) TEM image and particle size distribution of the PS latex from run 1. See Table 1 for detailed experimental conditions.

Influence of PEGMA concentration

The photopolymerizations were next conducted in the presence of different amounts of PEGMA, from 2.5 to 25 wt.% with respect to styrene (runs 1 and 4-7, Table 1). All final conversions were above 88% after *ca*. 24 h, most almost complete (Figure 4). The reaction rates at the beginning of the polymerization decreased with the PEGMA concentration (inset Figure 4), even drastically below 10% (runs 6 and 7). A similar trend has been observed in standard dispersion polymerizations.[33] Nevertheless, the final conversions still reached >90% conversion after 24 h. This showed that radicals were still generated over a long period, even if the initial rates were low.

As expected, a decrease in PEGMA concentration led to an increase of particle size (D_n) from 97 nm for 25 wt.% to 340 nm for 2.5 wt.%. Accordingly, the particle number decreased with decreasing the PEGMA concentration (Table 1). It should be noted that the particle size did however not exceed 345 nm, *i.e.*, a size similar to the maximum one observed in photoemulsion polymerizations.[17-18] The decrease of PEGMA concentration had a negative impact on the particle size distributions, with for example D_w/D_n = 1.09 at 18 wt.% of PEGMA while at 5 wt.% of PEGMA, D_w/D_n = 1.25 (Figure S4). As mentioned above, the obtention of broad PSDs for all samples may be due to the rather slow generation of radicals from our PIS resulting in a low and continuous nucleation, as shown by the evolution of particle number (N_p) with conversion (Figure S5).

The decrease in PEGMA concentration also led to a significant decrease of the molar masses from 104 000 g mol^{-1} for 25 wt.% to 32 000 g mol^{-1} for 2.5 wt.% (Table 1). Again this inverse correlation between particle size and molar mass has been observed and happens in most dispersion processes.[38] This could indicate that the number of radicals per particle is larger when the particle size increases, which triggers more termination reactions and lead to lower polymerization rates.

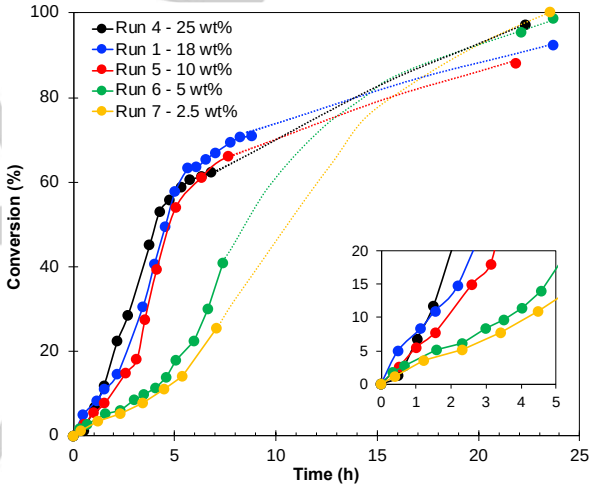

Figure 4. Evolution of conversion with time for dispersion photopolymerization of styrene for different amounts of stabilizer: 25 (black curve), 18 (blue curve), 10 (red curve), 5 (green curve) and 2.5 (orange curve) wt.% of PEGMA. See Table 1 for experimental details.

Influence of the PIS: three-component system versus disulfide only

In our previous studies,[17-18] we showed that the thiyl radicals generated from the homolytic cleavage of the S–S bond under visible light led to efficient emulsion polymerization of MMA, but not styrene. The combination of a greater MMA solubility in water and a k_p value higher than for styrene was put forward to explain the observations. This outcome is a further example of a photopolymerization where the optimal irradiation wavelength for initiation is not necessarily that of the maximal absorption, as first reported by Barner-Kowollik and coworkers.[39-40]

We therefore decided to test the disulfide as sole photoinitiator in the dispersion photopolymerization. We used a benchmark concentration of PEGMA at 18 wt.% of PEGMA (run 8, Table 1). Contrary to what was observed in emulsion conditions, the disulfide alone is capable of photoinitiating the polymerization of styrene. However, the latter needs more time to start with the disulfide alone (Figure 5a). While the retardation effect can be

attributed to the poor absorption of visible light by the disulfide which produces less radicals than the specially conceived full PIS (Figure S1c), the fact that the polymerization proceeds is the result of a higher available styrene concentration, since dispersion polymerizations start in an homogeneous phase. However, the rate was significantly faster after 4 h of reaction. After 8 h, monomer conversion reached 82% with the disulfide, but was only 70% with the full PIS. A stronger auto-acceleration was observed after 4 h, likely the result of a gel effect, explaining the higher molar mass obtained in this system (compare M_n = 200 kg mol^{-1} with M_n = 91 kg mol^{-1}). Also, in the full PIS, the NHC-borane allows transfer to the co-initiator, which can also moderate the chain lengths.[41]

Gratifyingly, the disulfide led to much larger PS particles (D_n = 337 nm) with a narrower particle size distribution (D_w/D_n = 1.02, Figure 5b). Since the disulfide alone generates less initiating radicals, it likely leads to the formation of less precursor particles. The nuclei are not immediately stabilized because less poly(styrene-*co*-PEGMA) graft copolymers are formed since less PS oligomers are produced. Therefore, the particles are larger. With the disulfide, after a first increase until ca. 20% conversion, the particle number is relatively constant throughout the polymerization, while that is not the case with the full PIS (Figure S6). All *nuclei* thereby grow to more uniform final particle sizes, as the rate of radical generation ensures a good balance between an efficient nucleation step and the adsorption of graft copolymers.

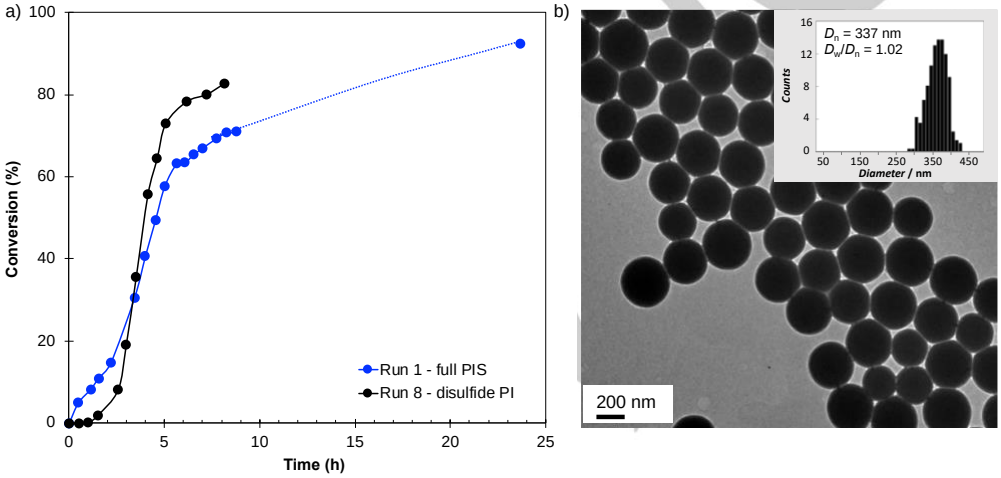

Figure 5. a) Evolution of conversion with time for dispersion photopolymerization of styrene for different PIS: our three-component PIS (run 1, blue curve) vs. disulfide alone (run 8, black curve). b) TEM image and particle size distribution of the PS latex from run 8. See Table 1 for experimental details.

Case of the full PIS at 10 wt.% PEGMA

As can be seen in Figure 4, at 10 wt.% PEGMA and below the polymerization profiles showed a much more pronounced delay. This led us to examine more closely what happens at 10 wt.%. To our surprise the reactions proved very stochastic (compare entries 5, 9 and 10 in Table 1), and we noticed important discrepancies. First, the auto-acceleration did not occur at the same time (see Figure 6, the dashed lines represent the hypothetic conversions as a function of time). The three curves show a nearly identical trend, but only for approximately the first 1.5 h of the synthesis. After that point, they develop randomly. Second, the particle sizes are similar for runs 5 and 10 (D_n = 207 and 202 nm, respectively, albeit with high dispersities), where the conversions are the highest (88%), but run 9 leads to a final conversion of only 56% after 23 h. A phenomenon seems thus to strongly impact the kinetic, sometimes limiting the conversion, but not the final particle size when the polymerization reaches high conversion.

This phenomenon was evident only at lower PEGMA concentration, since at 18 wt.% of PEGMA, the conversion curves were consistent (Figure 3a). Since higher PEGMA concentrations led to smaller particle sizes (D_n values around 150 nm), we surmised that when a critical size is reached and at relatively low conversions (between 0 and 10% – corresponding to objects around 130-140 nm diameter by DLS, see Figure S7), scattering affects the light penetration and therefore the radical initiation.

Chemtob and co-workers observed that the light was attenuated as soon as the polymer particles reach about 50 nm, even in the visible domain.[4] In our case, the 130-140 nm size reached at 10% conversion likely triggers scattering of the wavelengths needed to excite acridine orange. This leads to a drastic diminution of the production of radicals that can only be formed on the outer rim of the vessel, which affects the polymerizations.

The stochasticity is certainly a result of the broad particle size distributions caused by the continuous nucleation (Figure S8) already mentioned above at 18 mol% PEGMA. With a polydisperse population the critical size could be reached more quickly than with a monodisperse one. Nevertheless, the reactions still proceed, since stirring ensures the diffusion of these radicals through the reaction medium.

We next ran a conventional dispersion polymerization thermally initiated by AIBN at 70 °C (run 11). Even if a straightforward comparison of the radical flux generated by both types of initiation remains difficult, not least because the concentration of AIBN was about 4 times higher than that of the NHC-borane (5.7 10^{-3} M vs. 1.3 10^{-3} M, respectively), the polymerization initiated by AIBN did not experience the same lagging time and was much faster than the photoinitiated one (see inset in Figure 6). The particle size was

higher and the particle size distribution narrower (D_n = 246 nm and D_w/D_n = 1.02). Finally, a higher molar mass was obtained with AIBN (M_n = 116 000 g mol^{-1}) than with our PIS (around 60 000 g mol^{-1}). All these results are consistent with a better flux of radicals not limited by scattering, and the absence of potential H transfer from the NHC-borane.

The generation of radicals and the formation of larger particles seem therefore to be key factors at the origin of the stochasticity observed for the photopolymerization reactions in dispersion. When the particle population is polydisperse, the presence of even a small fraction of larger particles can strongly influence the light scattering and therefore the conversion. Nonetheless, in the end high conversions and stable latexes are always observed.

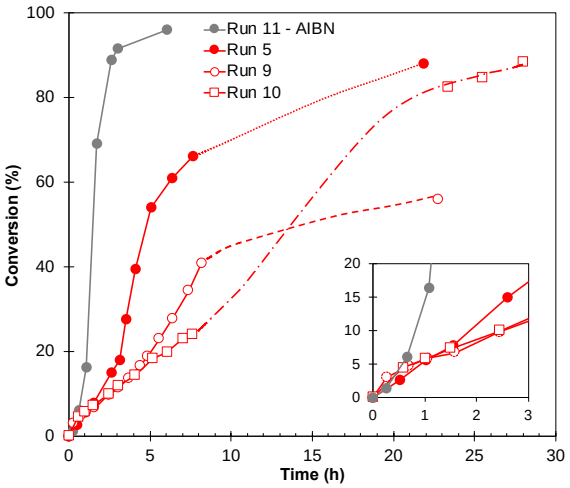

Figure 6. Reproducibility – Evolution of conversion with time for dispersion polymerization of styrene with the stabilizer PEGMA (10 wt.% with respect to styrene) under visible light (runs 5, 9 and 10) and thermally induced (run 11). See Table 2 for experimental details.

Influence of the addition of an organic base: TBAH

One factor that could impact the polymerization rate is a partial solubility of dicarboxylic acid diphenyl disulfide **2** in the hydroalcoholic mixture. Indeed, without the addition of a base, the disulfide can likely partition between the continuous phase and the monomer-swollen particles. We thus decided to examine how the introduction of tetrabutylammonium hydroxide (TBAH) would influence the reaction outcome. It is likely that the deprotonation will shift the partitioning of the disulfide towards the continuous phase and thus improve the photoinitiation there. All the syntheses were carried out at PEGMA 18 wt.% with a solids content of 10 wt.%, and a constant concentration of the three-component PIS (Table 2).

The final conversions were high for all TBAH concentrations tried (Figure 7a). The polymerization rates are all similar within the first ca. 1.5 h (inset in Figure 7a), and they are also similar to what happened without TBAH. The polymerization rate was highest for a TBAH concentration of 2.5 mM. The addition of more TBAH, *i.e.* 5 mM, led to a decrease of the polymerization rate.

Given that the first hour likely corresponds to the nucleation stage, which happens when the mixture is homogeneous, the first observation indicates that TBAH did not impact the nucleation itself. However, once the particles formed, the higher polymerization rate observed when TBAH is used can likely be attributed to a higher availability of the disulfide in the continuous phase, leading to a higher production of oligoradicals, which can enter into the growing particles. The polymerization rate drop with more TBAH might be attributed to the reduction of the acridine orange reactivity at more basic pH.

Very interestingly, we also observed an improvement of the size dispersity when the TBAH concentration increased (D_w/D_n = 1.09 without TBAH, and 1.02 for 2.5 and 5 mM). We can reasonably assume that the higher production of radicals in the continuous phase leads to a better involvement of PEGMA in particle stabilization, which is illustrated by a less pronounced increase of

Table 2. Visible-Light Dispersion Photopolymerizations of Styrene with the NHC-Borane-Based PIS in the presence of the organic base TBAH.

Entry[a]	[TBAH] (mmol L^{-1})	PEGMA (wt.%)	Time (h)	Conv. (%)	D_h (nm) [b]	PdI[b]	N_p (10^{13} cm^{-3}) [c]	D_n (nm) [d]	D_w/D_n [d]	N_p (10^{13} cm^{-3}) [e]	M_n (kg mol^{-1}) [f]	$Đ$ [f]
12	1.25	18	24.1	84	131	0.02	5.7	130	1.07	5.8	144	5.9
13	2.5	18	30	98	164	0.02	3.4	171	1.02	3.0	127	3.4
14	5	18	30	89	190	0.10	1.7	196	1.02	1.6	129	4.5
15	2.5	18	31	98	183	0.03	2.4	183	1.03	2.4	126	4.0
16	2.5	15	31.1	92	197	0.04	1.8	207	1.01	1.6	117	5.5
17	2.5	10	30.1	92	239	0.04	0.9	253	1.03	0.8	97	6.3
18	2.5	5	30.2	81	368	0.04	0.2	358	1.02	0.3	101	6.7
19 [g]	2.5	18	30.1	90	238	0.05	1.0	250	1.01	0.8	260	4.7

[a] Conditions: the continuous phase was prepared by adding styrene (10 wt.% with respect to water and ethanol), the stabilizer (PEGMA), NHC-borane (1.3 10^{-3} mol L^{-1}), the organic base TBAH, AO (1.3 10^{-5} mol L^{-1}, 1 mol%/NHC-BH$_3$), disulfide (6.3 10^{-4} mol L^{-1}, 50 mol%/NHC-BH$_3$) in ethanol/water (70/30 wt/wt). [b] Hydrodynamic diameter and polydispersity index determined by DLS. [c] Number of particles calculated from D_h. [d] Number-average diameter and size dispersity determined by TEM. [e] Number of particles calculated from D_n. [f] Number-average molar mass and dispersity determined by SEC-THF. [g] Same conditions as run 13 except without NHC-borane and without AO.

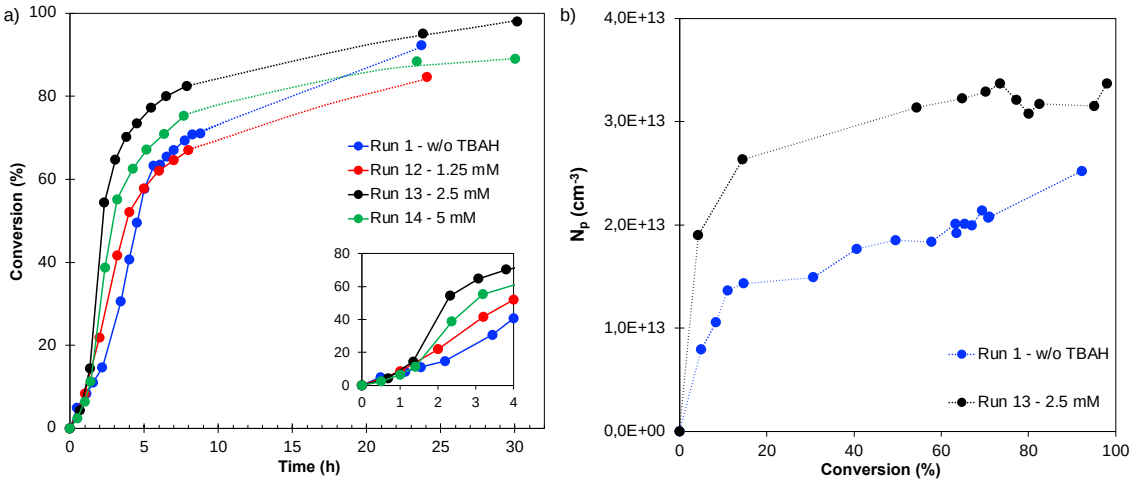

Figure 7. Evolution of a) conversion with time and b) particle number with conversion for dispersion photopolymerization of styrene carried out with 18 wt.% PEGMA and different concentration of TBAH: 0 (Run 3), 1.25 (Run 12), 2.5 (Run 13) and 5 mmol L^{-1} (Run 14). See Table 2 for experimental details.

the particle number above 10% conversion (Figure 7b). The increase in TBAH concentration also led to an increase of particle size, from D_n = 130 nm at 1.25 mM to 196 nm at 5 mM (Table 2 and Figure S9). One possible explanation may lie in the solubility of the PEG chains with respect to TBAH concentration. Indeed, the presence of salts could negatively affect the PEG solubility in the continuous phase (*via* a salting-out effect[42-44]) and consequently, the resulting graft copolymer would be less efficient for particle stabilization resulting in larger particles, with narrower size distributions.

After checking that the experiment at 2.5 mM was reproducible (Run 15, Table 2 and Figure S10), the PEGMA concentration with respect to styrene was varied from 18 to 5 wt.%, in the presence of TBAH (Table 2 and Figure 8, runs 13, 16-18). With 18 wt.% PEGMA the monomer conversion reached 98% after 30 h, whereas it was only 81% at 5 wt.% PEGMA for the same reaction time (with a slight inhibition of about an hour). Nevertheless, the polymerizations were always faster in the presence of TBAH and the stochasticity observed in the absence of TBAH was much reduced.

Lowering the PEGMA concentration led to an increase of the particle sizes, from ~170 nm at 18 wt.% to ~360 nm at 5 wt.% (Figure S11). Most importantly narrower PSDs were systematically obtained (D_w/D_n close to 1.02 *versus* 1.10-1.25 without TBAH). Moreover, the molar mass decreases only slightly with decreasing PEGMA concentrations, from 127 000 to ca. 100 000 g mol^{-1}. These molar masses are higher than in the absence of TBAH, especially at low PEGMA concentration (eg. 101 000 g mol^{-1} vs. 40 000 g mol^{-1} at 5 wt.% of PEGMA with and without TBAH, respectively runs 18 and 6).

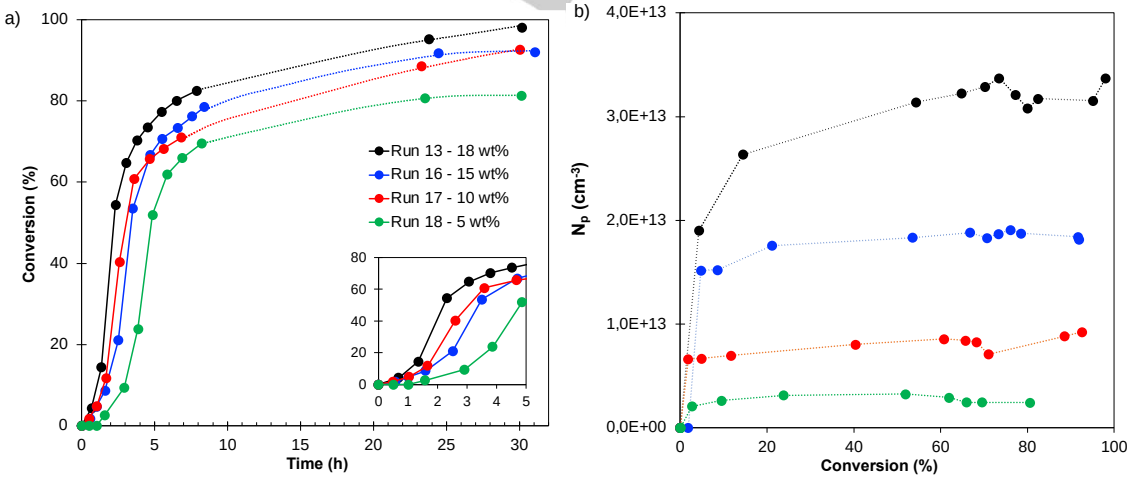

Figure 8. Evolution of a) conversion with time and b) particle number with conversion for dispersion photopolymerization of styrene for different amounts of PEGMA in the presence of TBAH at 2.5 10-3 mmol L-1: 18 (run 13), 15 (run 16), 10 (run 17) and 5 (run 18) wt.% with respect to styrene. See Table 2 for experimental details.

As mentioned above, it can be reasonably assumed that in the presence of TBAH, a higher number of radicals is generated in the continuous phase, which leads to faster polymerization rates. The comparison of the two experiments performed with 5 wt.% of PEGMA with and without TBAH – where the particle sizes are similar but the PSD significantly different – validates our previous hypothesis/observation that the particle size distribution greatly influences the polymerization rates, likely because it affects the light penetration. Broad distributions generate stochasticity because the random formation of larger objects affects the light penetration and hence the flux and capture of the initiating radicals.

When the disulfide was used as sole photoinitiator in the presence of TBAH (run 19, Table 2) the polymerization was faster and conversion reached 90% (Figure 9). However, the particles were now smaller than in the absence of TBAH (D_n = 250 nm vs. D_n = 337 nm – see run 8) and with a narrow size distribution. The molar masses obtained were the highest (M_n = 260 kg mol^{-1} vs. 200 kg mol^{-1} without TBAH).

The kinetic observations are consistent with what has been observed on the full PIS, suggesting TBAH acts in the same way as above. The real difference comes from the smaller particles sizes obtained, which is an opposite trend compared to the full PIS. It is possible that the higher concentration of initiating thiyl radicals in the continuous phase increases the chances of addition to PEGMA to form graft copolymers, hence resulting in better stabilization, all the more efficient since the deprotonated carboxylates may also participate.

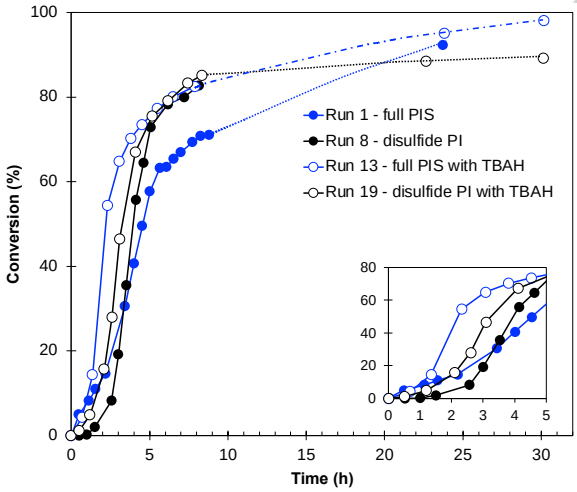

Figure 9. Conversion curves as a function of time for the full PIS vs. disulfide alone, with or without the presence of TBAH (2.5 mM) at 18 wt.% of PEGMA with respect to styrene. See Tables 1 and 2 for experimental conditions.

Particle stabilization with PVP

The use of PVP as a stabilizer in dispersion polymerization of styrene can lead to micrometric particles[38, 45] where PEGMA leads to smaller particles in hydroalcoholic media.[26, 33, 46-48] This is attributed to the stabilization mechanism associated to each macromolecule. PVP participates to particle stabilization *via* chain transfer reactions triggered by hydrogen atom abstraction from the PVP chain, leading to PS-grafted PVP, while – as described above – PEGMA is involved in the propagation step as co-monomer. It is well known that only a small fraction of PVP is involved in the particle stabilization. We therefore decided to use PVP40 (*ca.* 40 000 g mol^{-1}, Table 3) in our system.

The dispersion photopolymerization of styrene was carried out using our three-component PIS with 10 wt.% of PVP (runs 20-22, Figure 10). All the latexes were stable without any coagulum. However, a stochastic behavior was again observed after ca. 5 h, and the polymerizations plateaued at high conversions – albeit lower than with PEGMA (70-83%). Experimentally, we noticed that at the 5 h mark the reaction medium became very turbid, much more than with PEGMA. DLS showed that this corresponds to an average particle size of ~380 nm, *i.e.* again a critical particle size where scattering of the incident photons becomes predominant.

Table 3. Visible-Light Dispersion Photopolymerizations of Styrene using PVPK-30 as Stabilizer.

Run [a]	PVP (wt.%)	Time (h)	Conv. (%)	D_n (nm) [b]	D_w/D_n [b]	N_p (10^{11} cm^{-3}) [c]
20	10	30.4	71	859	1.001	1.7
21	10	24.3	69	794	1.006	2.2
22	10	23.2	83	766	1.002	2.9
23 [e]	10	6.4	100	931	1.005	1.8
24 [f]	10	25.4	72	1 006	1.014	1.0
25 [f]	10	28.9	72	925	1.008	1.4
26 [f]	5	23.7	58	1 212	1.063	0.5

[a] Conditions: the continuous phase was prepared by adding styrene (10 wt.% with respect to water and ethanol), the stabilizer (PVP), NHC-borane (1.3 10^{-3} mol L^{-1}), AO (1.3 10^{-5} mol L^{-1}, 1 mol%/NHC-BH$_3$), disulfide (6.3 10^{-4} mol L^{-1}, 50 mol%/NHC-BH$_3$) in ethanol/water (70/30 wt/wt). [b] Number-average diameter and size dispersity determined by TEM. [c] Number of particles calculated from D_n. [d] Number-average molar mass and dispersity determined by SEC-THF. [e] Thermal initiation with AIBN, 1 wt.%/styrene at 70 °C. [f] Same conditions as run 20 controlling the temperature at 50 °C instead of 40 °C.

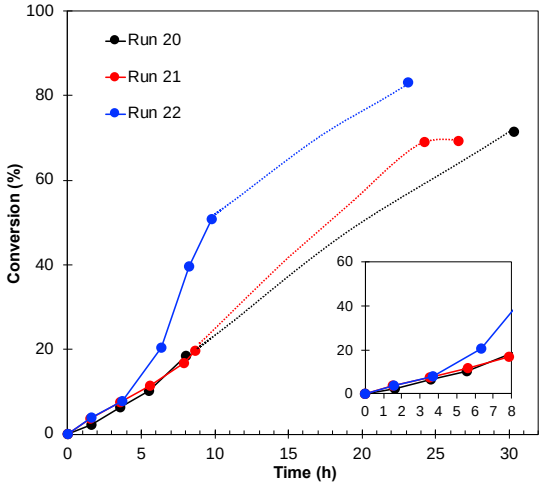

Figure 10. Reproducibility – Evolution of conversion with time for dispersion photopolymerization of styrene with 10 wt.% of PVP40 as stabilizer. See Table 3 for experimental conditions.

The good news was that the 300ish ceiling was broken for the first time (ca. 760-860 nm) and with very narrow distributions (Table 3 and Figures 11a and S12). Logically, the particle number was significantly lower than with PEGMA (about 100 times less). The sizes obtained were similar to what was obtained under regular thermal conditions with the same stabilizer (930 nm, run 23). As with PEGMA before, the polymerization still proceeds after the critical threshold is reached, only that there is a measure of randomness in the conversion transition.

As mentioned above, some PS oligoradicals terminate by chain transfer to PVP, thus generating initiating PVP macroradicals from which PS segments can grow. The resulting graft copolymers become insoluble in the continuous phase and adsorb on the particles. We believe that not enough graft copolymers are generated to stabilize the precursor particles during the nucleation step. The latter likely aggregate to form larger particles until they can be stabilized by the few amounts of the graft copolymer.

Higher temperatures have been shown to favor the formation of larger particles because PVP-*g*-PS graft copolymers are more soluble in the medium and as a consequence adsorb more slowly onto the precursor particles to stabilize them.[45, 49-50] We therefore repeated the photopolymerizations at 50 °C (runs 24 and 25). Stable latexes were again formed without any coagulum, and identical conversions (72%) were obtained after the stochastic phase, which started after 3.5 h (< 10% monomer conversion, Figure 12 – 250 nm by DLS). Nevertheless, micrometer-sized particles were obtained with narrow particle size distributions (Table 3 and Figures 11b and S13), a threshold that was pushed even further to 1.2 µm when less PVP was used (run 26, Figures 11c and S13). To the best of our knowledge, this is to date the highest particle size achieved so far using a photopolymerization in dispersed medium system.

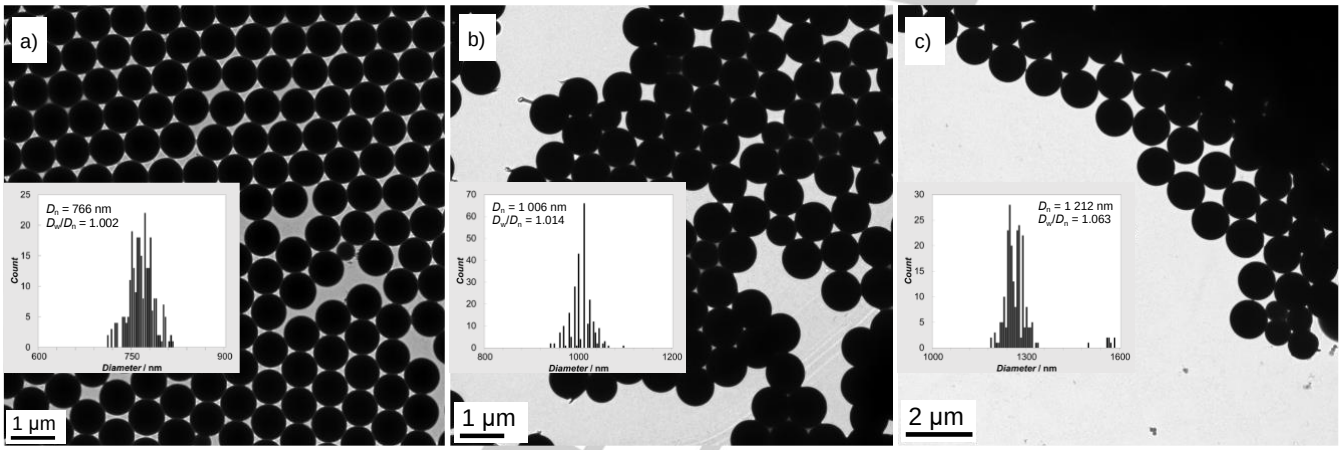

Figure 11. TEM images and particle size distributions of the PS latexes obtained with the full PIS using different PVP content (with respect to styrene): a) and b) 10 wt.% (runs 22 and 24), and c) 5 wt.% (run 26).

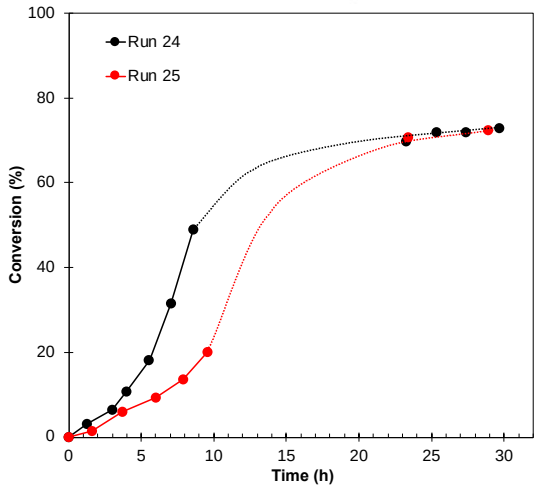

Figure 12. Reproducibility – Evolution of conversion with time for dispersion photopolymerization of styrene with 10 wt.% of stabilizer PVP 10 wt.% at 50 °C. See Table 3 for experimental conditions.

Conclusion

Stable PS latexes were synthesized in hydroalcoholic media under dispersion polymerization conditions under visible light irradiation, both using a three-component photoinitiating system based on a NHC-Borane, or using a single disulfide.

The use of PEGMA as a reactive stabilizer led to broad size distributions in comparison with thermally activated dispersion polymerizations, and to a stochastic kinetic behavior, which we attributed to a critical particle size (~140 nm), at which light penetration within the reaction medium and radical initiation were negatively impacted, a feature made worse by the particle size polydispersity. It is important to note that the growing opacity of the reaction medium did not prevent radical formation, as the systems reached full conversion. The addition of an organic base (TBAH) ended the stochasticity and enabled faster photopolymerizations with narrow size distributions. TBAH likely

improves the disulfide solubility in the hydroalcoholic medium, leading to a higher production of initiating radicals, associated to a better involvement of PEGMA in particle stabilization.
In addition, in the presence of TBAH, an increase of the particle sizes was observed, albeit the average sizes remained at the ~300-350 nm ceiling that we also encountered under emulsion polymerization conditions. With the full PIS, TBAH likely negatively affects the PEG solubility in the continuous phase (salting out effect) resulting in a less efficient stabilization of the particles by the graft copolymer. For the disulfide PI, with and without TBAH, the inefficient decomposition of the disulfide because of its low absorption in the visible range likely leads to a retardation of the nucleation and thus to a weak probability to generate graft copolymers, and as a result to the production of fewer and larger particles.
Gratifyingly, the use of PVP as stabilizer led to very large particles – up to 1.2 µm – with very narrow particle size distributions. The polymerization kinetics again went through a stochastic phase, this time at a larger critical size (380 nm). Having a narrow size distribution of the growing objects is a key requirement to obtain large particles. The production of such large latex particles by photoinitiated polymerizations has never been observed before.

Acknowledgements

The authors acknowledge the financial support from the Agence Nationale de la Recherche (Photo-B, ANR-16-CE07-0032 & IR-Emulsion ANR-20-CE06-0009). Magalie Schoumacker (CP2M/LHCEP) is acknowledged for her technical support.

Keywords: Photopolymerization • Dispersion • Visible light • Radicals • Photochemistry

[1] H. Lai, J. Zhang, F. Xing, P. Xiao, *Chem. Soc. Rev.* **2020**, *49*, 1867-1886.
[2] L. Delafresnaye, F. Feist, J. P. Hooker, C. Barner-Kowollik, *Nat. Commun.* **2022**, *13*, 5132.
[3] C. M. Q. Le, G. Schrodj, I. Ndao, B. Bessif, B. Heck, T. Pfohl, G. Reiter, J. Elgoyhen, R. Tomovska, A. Chemtob, *Macromol. Rapid Commun.* **2022**, *43*, 2100740.
[4] F. Jasinski, P. B. Zetterlund, A. M. Braun, A. Chemtob, *Prog. Polym. Sci.* **2018**, *84*, 47-88.
[5] M. Takeishi, H. Yoshida, S. Niino, S. Hayama, *Makromol. Chem.* **1978**, *179*, 1387-1391.
[6] N. J. Turro, M.-F. Chow, C.-J. Chung, C.-H. Tung, *J. Am. Chem. Soc.* **1980**, *102*, 7391-7393.
[7] A. Merlin, J.-P. Fouassier, *J. Polym. Sci. Polym. Chem. Ed.* **1981**, *19*, 2357-2359.
[8] K. Krüger, K. Tauer, Y. Yagci, N. Moszner, *Macromolecules* **2011**, *44*, 9539-9549.
[9] M. Ratanajanchai, D. Tanwilai, P. Sunintaboon, *J. Colloid Interface Sci.* **2013**, *409*, 25-31.
[10] K. Shen, Y. Jiang, Z. Liu, D. Qi, H. Wang, Y. Li, *Macromol. Chem. Phys.* **2015**, *216*, 1990-1996.
[11] Z. Huang, T. Qiu, H. Xu, H. Shi, J. Rui, X. Li, L. Guo, *Macromolecules* **2018**, *51*, 7329-7337.
[12] Q. Cao, T. Heil, B. Kumru, M. Antonietti, B. V. K. J. Schmidt, *Polym. Chem.* **2019**, *10*, 5315-5323.
[13] W. Fan, M. Tosaka, S. Yamago, M. F. Cunningham, *Angew. Chem. Int. Ed.* **2018**, *57*, 962-966.
[14] X. Su, Y. Jiang, P. G. Jessop, M. F. Cunningham, Y. Feng, *Macromolecules* **2020**, *53*, 6018-6023.
[15] J. Yeow, C. Boyer, *Adv. Sci.* **2017**, *4*, 1700137.
[16] V. Tkachenko, C. Matei Ghimbeu, C. Vaulot, L. Vidal, J. Poly, A. Chemtob, *Polym. Chem.* **2019**, *10*, 2316-2326
[17] F. Le Quéméner, D. Subervie, F. Morlet-Savary, J. Lalevée, M. Lansalot, E. Bourgeat-Lami, E. Lacôte, *Angew. Chem. Int. Ed.* **2018**, *57*, 957-961.
[18] D. Subervie, F. Le Quéméner, R. Canterel, P.-Y. Dugas, O. Boyron, J. Lalevée, E. Bourgeat-Lami, M. Lansalot, E. Lacôte, *Macromolecules* **2021**, *54*, 2124-2133.
[19] S. Kawaguchi, K. Ito, in *Polymer Particles, Vol. 175* (Ed.: M. Okubo), Springer Berlin Heidelberg, Berlin, Heidelberg, **2005**, pp. 299-328.
[20] J. Chen, Z. Zeng, J. Yang, Y. Chen, *J. Polym. Sci., Part A: Polym. Chem.* **2008**, *46*, 1329-1338.
[21] Z. Huang, F. Sun, S. Liang, H. Wang, G. Shi, L. Tao, J. Tan, *Macromol. Chem. Phys.* **2010**, *211*, 1868-1878.
[22] Z. Zhu, F. Sun, L. Yang, K. Gu, W. Li, *Chem. Eng. J.* **2013**, *223*, 395-401.
[23] P. B. Zetterlund, S. C. Thickett, S. Perrier, E. Bourgeat-Lami, M. Lansalot, *Chem. Rev.* **2015**, *115*, 9745–9800.
[24] N. J. W. Penfold, J. Yeow, C. Boyer, S. P. Armes, *ACS Macro Lett.* **2019**, *8*, 1029-1054.
[25] F. D'Agosto, J. Rieger, M. Lansalot, *Angew. Chem. Int. Ed.* **2020**, *59*, 8368-8392.
[26] I. Capek, M. Riza, M. Akashi, *Makromol. Chem.* **1992**, *193*, 2843-2860.
[27] I. Capek, M. Riza, M. Akashi, *Eur. Polym. J.* **1995**, *31*, 895-902.
[28] P. Lacroix-Desmazes, A. Guyot, *Colloid Polym. Sci.* **1996**, *274*, 1129-1136.
[29] P. Lacroix-Desmazes, A. Guyot, *Polym. Bull.* **1996**, *37*, 183-189.
[30] P. Lacroix-Desmazes, A. Guyot, *Polym. Adv. Technol.* **1997**, *8*, 608-615.
[31] P. Lacroix-Desmazes, A. Guyot, *Polym. Adv. Technol.* **1997**, *8*, 601-607.
[32] K. E. J. Barrett, H. R. Thomas, *J. Polym. Sci., Part A-1: Polym. Chem.* **1969**, *7*, 2621-2650.
[33] I. Capek, M. Riza, M. Akashi, *J. Polym. Sci., Part A: Polym. Chem.* **1997**, *35*, 3131-3139.
[34] J. Liu, C. H. Chew, S. Y. Wong, L. M. Gan, J. Lin, K. L. Tan, *Polymer* **1998**, *39*, 283-289.
[35] S. Kobayashi, H. Uyama, J. H. Choi, Y. Matsumoto, *Polym. Int.* **1993**, *30*, 265-270.
[36] P. Lacroix-Desmazes, A. Guyot, *Macromolecules* **1996**, *29*, 4508-4515.
[37] K. Ito, H. Tsuchida, A. Hayashi, T. Kitano, E. Yamada, T. Matsumoto, *Polym. J.* **1985**, *17*, 827-839.
[38] A. J. Paine, W. Luymes, J. McNulty, *Macromolecules* **1990**, *23*, 3104-3109.
[39] D. E. Fast, A. Lauer, J. P. Menzel, A.-M. Kelterer, G. Gescheidt, C. Barner-Kowollik, *Macromolecules* **2017**, *50*, 1815-1823.
[40] I. M. Irshadeen, S. L. Walden, M. Wegener, V. X. Truong, H. Frisch, J. P. Blinco, C. Barner-Kowollik, *J. Am. Chem. Soc.* **2021**, *143*, 21113-21126.
[41] B. Aubry, R. Canterel, M. Lansalot, E. Bourgeat-Lami, A. Airoudj, B. Graff, C. Dietlin, F. Morlet-Savary, J. Blahut, L. Benda, G. Pintacuda, E. Lacôte, J. Lalevée, *Angew. Chem. Int. Ed.* **2021**, *60*, 17037-17044.
[42] S. Saeki, N. Kuwahara, M. Nakata, M. Kaneko, *Polymer* **1977**, *18*, 1027-1031.
[43] J. P. Magnusson, A. Khan, G. Pasparakis, A. O. Saeed, W. Wang, C. Alexander, *J. Am. Chem. Soc.* **2008**, *130*, 10852-10853.
[44] F. E. Bailey, R. W. Callard, *J. Appl. Polym. Sci.* **1959**, *1*, 56-62.
[45] A. J. Paine, *Macromolecules* **1990**, *23*, 3109-3117.
[46] I. Capek, M. Riza, M. Akashi, *Polym. J.* **1992**, *24*, 959-970.
[47] I. Capek, S. H. Nguyen, D. Berek, *Polymer* **2000**, *41*, 7011-7016.
[48] M.-Q. Chen, T. Serizawa, A. Kishida, M. Akashi, *J. Polym. Sci., Part A: Polym. Chem.* **1999**, *37*, 2155-2166.
[49] Y. Chen, H.-W. Yang, *J. Polym. Sci., Part A: Polym. Chem.* **1992**, *30*, 2765-2772.
[50] H. Bamnolker, S. Margel, *J. Polym. Sci., Part A: Polym. Chem.* **1996**, *34*, 1857-1871.

Entry for the Table of Contents

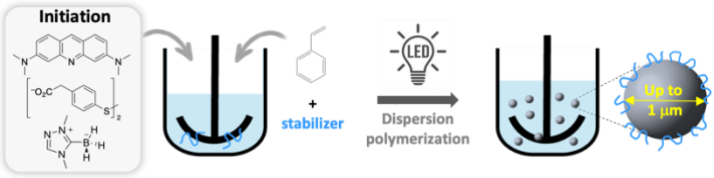

Styrene can be photopolymerized in dispersion using visible light and an optimized photo-initiating system, overcoming light scattering by the growing objects. Stable latexes with particle diameters up to 1.2 µm were obtained using poly(*N*-vinylpyrrolidone) as stabilizer. This represents a fourfold increase in the largest particle size ever reached by a photochemical process in a dispersed medium.

Institute and/or researcher Twitter usernames: @cp2m_lab; @LansalotMuriel